

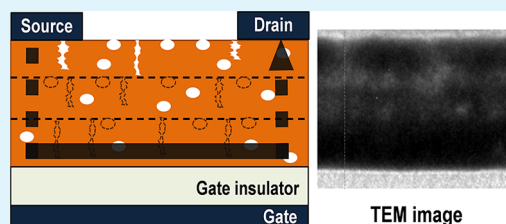
Improved Electrical Performance of an Oxide Thin-Film Transistor Having Multistacked Active Layers Using a Solution Process

Deuk Jong Kim, Dong Lim Kim, You Seung Rim, Chul Ho Kim, Woong Hee Jeong, Hyun Soo Lim, and Hyun Jae Kim*

School of Electrical and Electronic Engineering, Yonsei University, 50 Yonsei-ro, Seodaemun-gu, Seoul 120-749, Korea

ABSTRACT: Thin-film transistors (TFTs) with multistacked active layers (MSALs) have been studied to improve their electrical performance. The performance enhancement with MSALs has been attributed to higher film density in the effective channel; the density was higher because the porosities of the sublayers were reduced by filling with solution. The proposed TFT with MSALs exhibited an enhanced field-effect mobility of $2.17 \text{ cm}^2/(\text{V s})$ and a threshold voltage shift under positive bias stress of 8.2 V, compared to $1.21 \text{ cm}^2/(\text{V s})$ and 18.1 V, respectively, for the single active layer TFT.

KEYWORDS: thin-film transistor, solution process, multistacked active layer, effective channel thickness, density, porosity



1. INTRODUCTION

Oxide semiconductors (OSs) have received much attention because they can be applied to the active layer of thin-film transistor (TFT); they have higher mobility than a-Si, and have better electrical uniformity over a large area than poly-Si.¹ One representative OS material, indium–gallium–zinc oxide (IGZO), is the active material in large-area displays.^{2,3} Recently, many groups have explored solution-processing of OSs because this approach has the advantages of lower manufacturing costs,⁴ good control of material composition,⁵ and ease of fabrication on large or flexible substrates.⁶ However, solution-processed TFTs have inferior transfer characteristics and reliabilities compared to vacuum-processed TFTs. Research groups have tried to improve these inferior properties by modifying the heat-treatment conditions,^{7,8} the combination of additional materials,⁹ and engineering the precursors.¹⁰ However, those techniques faced an inherent limitation of solution-processed films, i.e., low film density because of porosities such as pores and pin-holes that were created by solvent volatilization.^{11,12} It was expected that a reduction of film porosity would improve the performance of solution-processed TFTs. In this paper, the improved electrical performance of the IGZO TFTs made by the solution process was investigated. The multistacked layers had lower porosity and higher density than the single layer, and the enhanced film density of the active layer was expected to improve the electrical performance. We have proposed an explanation for the lower film porosity in stacked solution-processed thin films and a mechanism for the improved TFT performance.

2. EXPERIMENTAL PROCEDURE

The solutions for the IGZO active material were prepared by dissolving indium nitrate hydrate [$\text{In}(\text{NO}_3)_3 \cdot x\text{H}_2\text{O}$], gallium nitrate hydrate [$\text{Ga}(\text{NO}_3)_3 \cdot x\text{H}_2\text{O}$] and zinc acetate [$\text{Zn}(\text{CH}_3\text{COO})_2 \cdot 2\text{H}_2\text{O}$] in 2-methoxyethanol. The In:Ga:Zn mole ratio was 5:1:2. The solution

was prepared at 0.1, 0.3, and 0.5 M to evaluate the film density and the thickness as functions of molarity. To fabricate bottom-gate TFTs, the prepared solutions were spin-coated at 3000 rpm for 30 s onto heavily doped p-type Si wafers, upon which a 1200 Å thick SiO_2 layer was grown. The coated IGZO films were prebaked for 5 min at 300 °C and then postannealed for 3 h at 450 °C. A TFT with multistacked active layers (MSALs) was fabricated by stacking multiple layers made from a 0.1 M solution. Spin-coating and pre- and postannealing were repeated as many times as the number of layers of MSALs. However, the entire postannealing time for single active layer (SAL) and MSALs was equal to 3 h. In the case of three-MSALs, the processes were repeated 3 times and each postannealing step was performed at 450 °C for 1 h. After deposition of the IGZO films, source and drain electrodes with a 200 nm thick Al were deposited by sputtering with a shadow mask. The channel was 1000 μm wide and 150 μm long. The density and the thickness of the IGZO films were analyzed by X-ray reflectivity (XRR) and field-emission scanning electron microscopy (FE-SEM), respectively. Transmission electron microscopy (TEM) was used to analyze the structure and density of the film. In order to analyze the film density through TEM image, Gatan Digital Micrograph software was used. The electrical properties were measured with a gate voltage (V_G) from -30 to 30 V and a drain voltage (V_D) of 10 V. The positive bias stress (PBS) was applied under a V_G of 20 V and a V_D of 10 V over 1000 s.

3. RESULTS AND DISCUSSION

3.1. Electrical Characteristics of the Single Active Layer TFTs. Figure 1 shows two key factors that affected the characteristics of the IGZO TFTs. When the molarity of the solution was changed to control the film thickness, the porosity of the film also changed. The threshold voltage (V_{TH}) of the sputtering-processed IGZO TFTs showed a continuous negative shift with increasing active layer thickness. This

Received: May 11, 2012

Accepted: July 13, 2012

Published: July 13, 2012

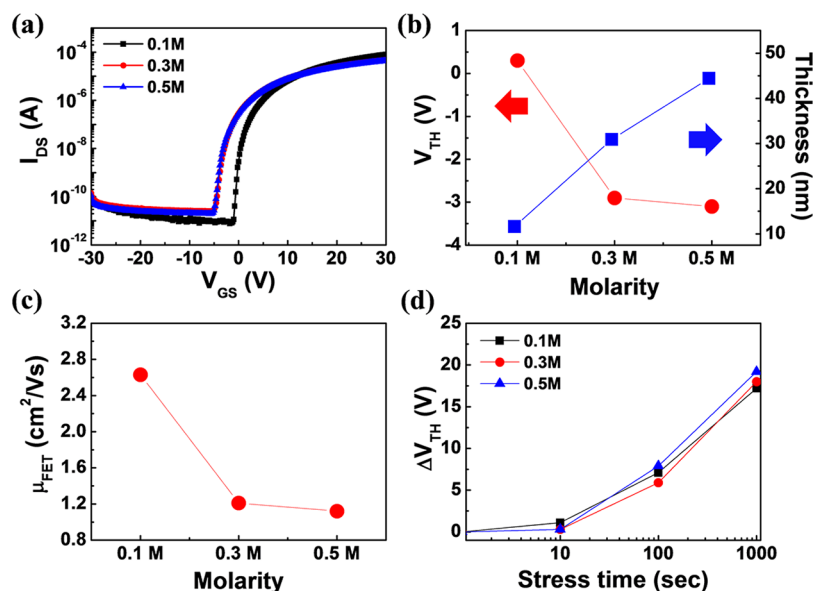


Figure 1. SAL TFT characteristics for different molarity: (a) transfer characteristics, (b) V_{TH} characteristics and the thickness of the active layer, (c) μ_{FET} characteristics, and (d) ΔV_{TH} characteristics under PBS.

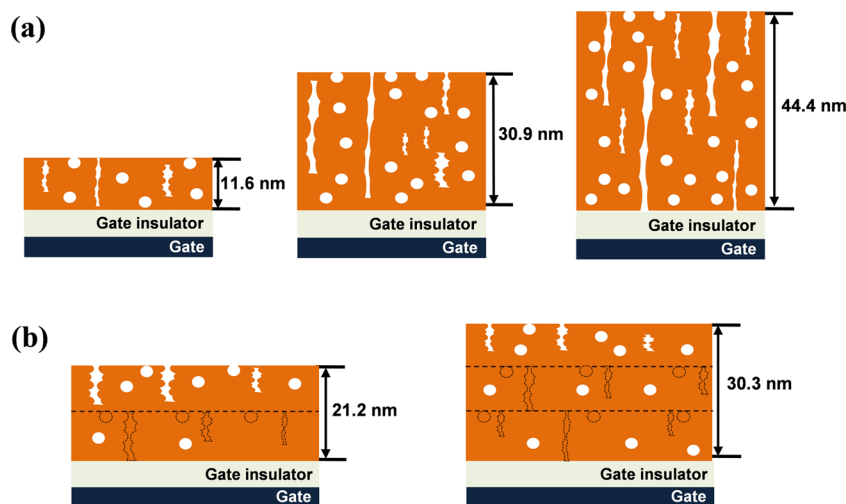


Figure 2. Cross-sectional diagrams of the active layer and the active thickness measured by SEM: (a) the single layer made with 0.1, 0.3, and 0.5 M solutions; (b) two- and three-multistacked layers made with a 0.1 M solution, and stacked, the interfacial pores and pin-holes in the sublayer filled by solution to form an upper layer.

phenomenon was attributed to increased free carrier accumulation in the channel region due to the larger volume of the active layer.^{13–15} For the solution-processed IGZO, the V_{TH} characteristic of a 0.3 M TFT was shifted to a more negative value than that for the 0.1 M TFT; in spite of the increased active thickness, the V_{TH} shift was difficult to observe for the 0.5 M TFT as shown in panels a and b in Figure 1. The carrier concentration for different molarity can be calculated with equation,¹⁶ $N_c = C_{ox}V_{TH}/qt_{active}$, where C_{ox} is the gate oxide capacitance per unit area, q is the elementary charge, and t_{active} is the active layer thickness. The calculated values for 0.1, 0.3, and 0.5 M are 4.4×10^{16} , 1.6×10^{17} , and 1.2×10^{17} cm⁻³, respectively. The carrier concentration of 0.5 M was lower than that of 0.3 M, which could be explained by the increased defect density due to the deterioration of film porosity.^{11–15} This result implied that the effective channel,¹⁶ where carriers accumulated by the gate electric field, was confined. Thus, the active layer above effective channel did not contribute to the

negative V_{TH} shift due to the defects in the film. Roughly considered the characteristic of the saturated V_{TH} , the effective channel thickness of the single active layer was about 30 nm (the active layer thickness of 0.3 M TFT). As shown in Figure 1c, the field-effect mobility (μ_{FET}) decreased with increasing molarity. This was because the thick film, fabricated with a high-molarity solution, had many defects to capture electrons and an increased carrier scattering related to the trap charges in the bulk.¹⁷ The reason for the increasing film porosity with increasing molarity is discussed below.

Figure 1d shows the reliability under a positive bias stress (PBS). The shift in V_{TH} of the sputtering-processed IGZO TFTs under PBS was affected by charge trapping.¹⁵ Field-induced adsorption of oxygen and desorption of H₂O at the surface also contributed to the V_{TH} shift; this shift depended on the active layer thickness.^{16,18,19} The solution-processed IGZO TFTs with the thin active layer made by a low-molarity solution had a poor PBS characteristic, which could be attributed to the

increased charge density²⁰ in the films and the increased back-surface effect due to the decreased active layer thickness. The TFT with the thick active layer made by a high-molarity solution exhibited not only poor PBS reliability but also poorer transfer characteristics. This was because the thicker active layers made with the 0.3 and 0.5 M solution had more defects in the bulk and interfaces than the thinner active layer fabricated with a 0.1 M solution. The defects could be affected by the pores and pin-holes in the active layer.^{11,12} The higher porosities of films made with the higher molarity solutions may have resulted from vaporization and condensation processes as shown in Figure 2a. Thus, to obtain enhanced electrical performance of solution-processed TFTs, a thick active layer must be fabricated by a low-molarity solution.

3.2. Analysis on the Structure of Active Layer. The surface of single and multistacked layer had many pores on the surface (not include in this paper), which were possibly formed during vaporization, decomposition, and condensation processes. Thus, the film made by a low-molarity solution could have higher density as shown in Figure 2a. To obtain a thick film with high density, we stacked multiple thin layers made from a 0.1 M solution because it had the best transfer characteristics in this experiment. The higher density of the multilayered film may be due to filling of the pin-holes and pore regions of the sublayers by the subsequent solution process as shown in Figure 2b. The film density could be changed with the quantity of pores and pin-holes. Thus, for estimating pores and pin-holes, the film density was analyzed by X-ray reflectivity (XRR).²¹ The measured XRR data for the IGZO films are shown in Figure 3. The 0.1 M film had a density of 5.34 g/cm³,

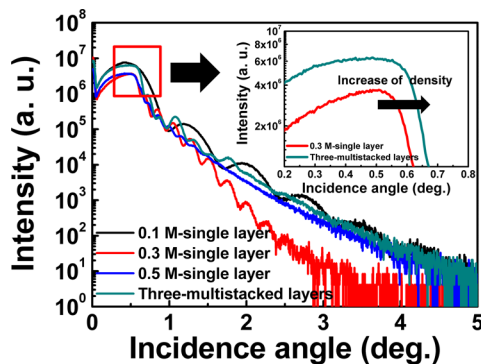


Figure 3. (a) Measured XRR data for the different molarity and active structure, (b) enlarged graph for the box area; single layer made with a 0.3 M solution and three-multistacked layers made with a 0.1 M solution.

whereas the films made by 0.3 and 0.5 M solution had densities of 4.51 and 4.45 g/cm³, respectively. This means that the film made by a low-molarity solution had higher density than the one made by a high-molarity solution. The three-multistacked layers had higher density than single layer made by a 0.3 M solution, which was estimated by considering a higher critical angle²¹ as shown in the inset of Figure 3. TEM was performed to analyze the film density and structure. The film density could be estimated by analyzing the transmitted electron intensity, which was extracted by TEM images. Figure 4 shows that the black regions have a higher density than the gray ones; the black region of the image is due to the lower transmitted electron intensity. Therefore, the multistacked layers with many black regions have higher density than single layer. Also, the

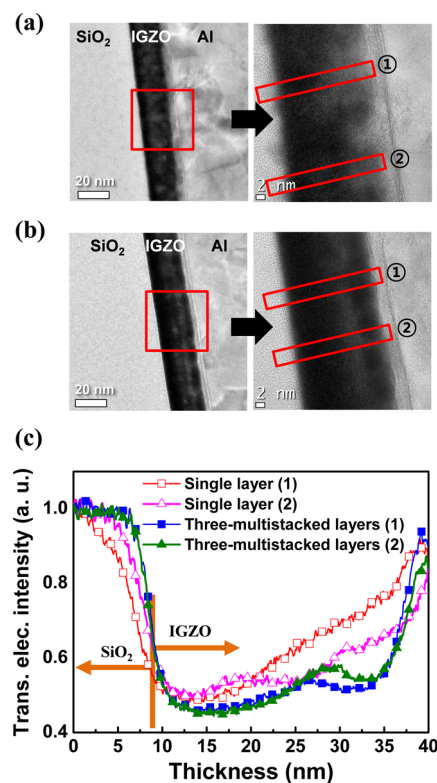


Figure 4. TEM images: (a) the single layer fabricated with a 0.3 M solution; (b) the multistacked layers fabricated by stacking three single layers, each made with a 0.1 M solution; and (c) the transmitted electron intensity obtained by Gatan Digital Micrograph.

sublayers have a higher density than the top layer. In addition, the middle-interfaces in the film are found as shown in the Figure 4b.

3.3. Electrical Characteristics of the Multistacked Active Layers TFTs. Interestingly, the V_{TH} values of the TFTs with MSALs differed from the TFTs with a SAL as shown in Figure 5a. The V_{TH} of the TFT with a SAL was negatively shifted by 3.5 V as the thickness increased from 11.6 to 44.4 nm; the TFT with MSALs was negatively shifted by only 1.5 V, even though the active layer was thicker (67.5 nm). The effective channel thickness of the SAL TFT was estimated at 30 nm based on the saturated V_{TH} shift of the 30 nm thick film made from a 0.3 M solution. The effective channel thickness of the MSALs TFTs was about 20 nm. This was because the V_{TH} values of the MSALs TFTs were between the value for the 0.1 M SAL TFT and that for the 0.3 M SAL TFT as shown in panels a and b in Figure 5. It appears that the carrier concentration that causes a negative V_{TH} shift did not increase beyond that for the 0.3 M SAL TFT, despite the higher film density and increased thickness.¹⁶ These transfer characteristics may be due to the formation of the middle-interfaces between the layers when the MSALs structure was prepared.²² The trap sites in the middle-interfaces contributed to the capture of free carriers, and the charge barrier formed by the trapped charge could weaken the gate electric field.^{20,22} Figure 5c shows how the μ_{FET} of MSALs TFTs changed with the number of active layers. The MSALs TFTs had a better μ_{FET} than the SAL TFT made with a 0.3 M solution. This was because the number of trap sites in the active layers were reduced as the film density increased via the multilayered structure as shown in Figure 6. However, as the number of

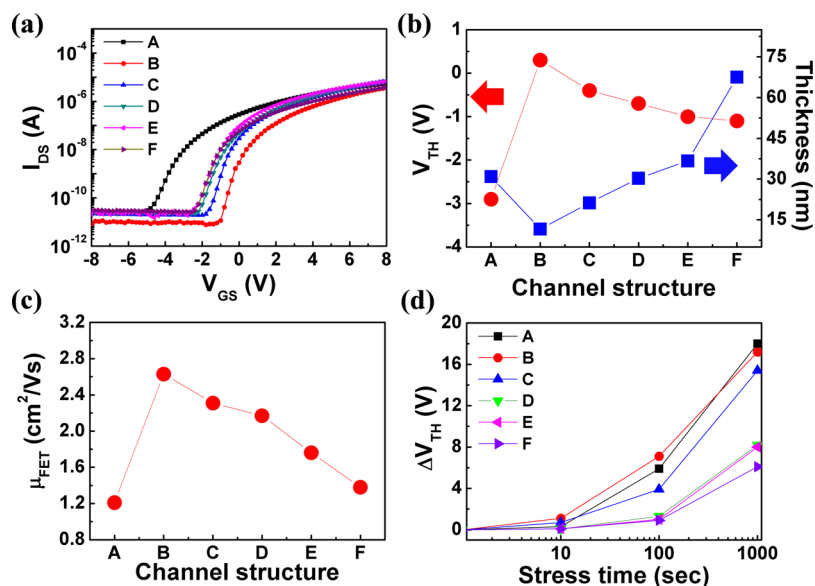


Figure 5. Characteristics of the MSALs TFTs as a function of the number of stacked layers. (A) the SAL made with a 0.3 M solution, (B) the SAL made with a 0.1 M solution, (C) two-MSALs made with a 0.1 M solution, (D) three-MSALs, (E) four-MSALs, and (F) six-MSALs: (a) transfer characteristics, (b) V_{TH} characteristics and the thickness of the active layer, (c) μ_{FET} characteristics, and (d) ΔV_{TH} characteristics under PBS.

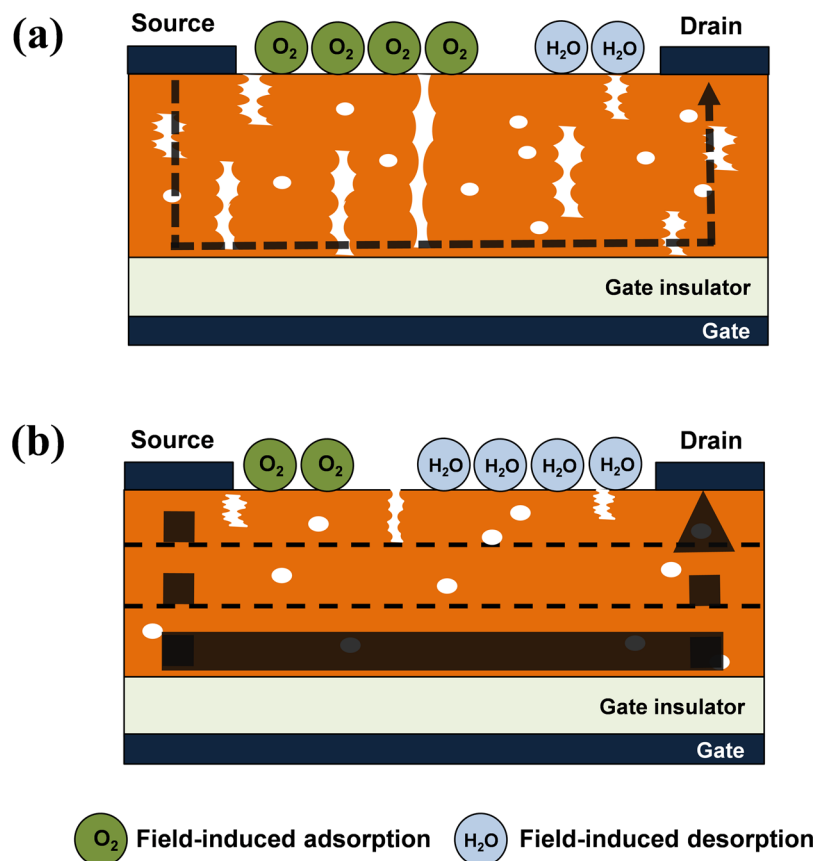


Figure 6. Schematic diagrams for (a) the TFT with SAL made from a 0.3 M solution, (b) the TFT with three-MSALs made from a 0.1 M solution.

active layers increased, the μ_{FET} decreased because of the increased resistance between IGZO channel and S/D electrodes with the increased active thickness;²³ it could be also affected by the increased number of trap sites and trap charges in the middle-interfaces.^{17,22}

The PBS reliability of the MSALs TFTs was better than that of the SAL TFT as shown in Figure 5d. The MSALs TFTs had

different properties, including higher film density, number of middle-interfaces, and increased active layer thickness with increasing number of stacked layers. The densities of the sublayers in the multilayered structure increased through filling of the pores and pin-holes with solution. The improved film density contributed to the reduction of the trap densities in the active layer as shown in Figure 6. Thus, the MSALs TFTs had

better PBS reliability as the number of active layers increased through the stacking process. We believe that the film density in the effective channel (about 20 nm) was the key factor for improving PBS reliability; the reliability dramatically improved from the three- and four-MSALs TFTs that had enhanced film densities in the region of the effective channel, but the reliability of the two-MSALs TFT was slightly better than that of the SAL TFT because of the porous second layer in the effective channel. The middle-interfaces contributed to the decrease in positive V_{TH} shift under PBS because the weakened gate electric field changed the distribution of the field-induced absorbed O_2 and desorbed H_2O at the back-surface by trapping negative charges in the middle-interfaces as shown in Figure 6.^{18–22} The increased active layer thickness also contributed to the enhanced PBS reliability by weakening the gate electric field. However, comparing ΔV_{TH} among the SAL, the three-MSALs, and the six-MSALs (Figure 5d), it seems that the film density in the effective channel is more important for PBS reliability than the back-surface effect which changed with increasing active layer thickness and the number of middle-interfaces.

4. CONCLUSION

In summary, to enhance the electrical performance of solution-processed TFTs, the defects in the active layers should be reduced, especially in the effective channel. Also, an active layer should have sufficient thickness to suppress the effect of the back-surface by the gate electric field. Thus, we adopted the TFT with MSALs to fabricate a thick film having enhanced film density and confirmed the improved TFT performance. Furthermore, the mechanism of the improvement was explained by the enhanced film density, the charge barrier in the middle-interfaces, and the increased active layer thickness. We found that the TFT having three-multistacked active layers was the optimal design.

AUTHOR INFORMATION

Corresponding Author

*E-mail: hjk3@yonsei.ac.kr.

Notes

The authors declare no competing financial interest.

ACKNOWLEDGMENTS

This work was supported by Samsung Mobile Display and the National Research Foundation of Korea (NRF) grant funded by the Korean Ministry of Education, Science and Technology (MEST) (2011-0028819).

REFERENCES

- (1) Kwon, J.-Y.; Lee, D.-J.; Kim, K. B. *Electron. Mater. Lett.* **2011**, *7*, 1–11.
- (2) Kamiya, T.; Nomura, K.; Hosono, H. *Sci. Technol. Adv. Mater.* **2010**, *11*, 044305.
- (3) Hsieh, H.-H.; Lu, H.-H.; Ting, H.-C.; Chuang, C.-S.; Chen, C.-Y.; Lin, Y. J. *Inf. Display* **2010**, *11*, 160–164.
- (4) Kim, G. H.; Shin, H. S.; Ahn, B. D.; Kim, K. H.; Park, W. J.; Kim, H. J. *J. Electrochem. Soc.* **2009**, *156*, H7–H9.
- (5) Sirringhaus, H. *Adv. Mater.* **2005**, *17*, 2411–2425.
- (6) Lee, D.-H.; Chang, Y.-J.; Herman, G. S.; Chang, C.-H. *Adv. Mater.* **2007**, *19*, 843–847.
- (7) Lee, C.-G.; Dodabalapur, A. *Appl. Phys. Lett.* **2010**, *96*, 243501.
- (8) Nomura, K.; Kamiya, T.; Hirano, M.; Hosono, H. *Appl. Phys. Lett.* **2009**, *95*, 013502.

- (9) Lim, J. H.; Shim, J. H.; Choi, J. H.; Joo, J.; Park, K.; Jeon, H.; Moon, M. R.; Jung, D.; Kim, H.; Lee, H.-J. *Appl. Phys. Lett.* **2009**, *95*, 012108.
- (10) Banger, K. K.; Yamashita, Y.; Mori, K.; Peterson, R. L.; Leedham, T.; Rickard, J.; Sirringhaus, H. *Nat. Mater.* **2011**, *10*, 45–50.
- (11) Li, C.-S.; Li, Y.-J.; Wu, Y.; Ong, B.-S.; Loutfy, R.-O. *J. Mater. Chem.* **2009**, *19*, 1626–1634.
- (12) Lee, D.-H.; Chang, Y.-J.; Stickle, W.; Chang, C.-H. *J. Electrochem. Soc.* **2007**, *10*, K51–K54.
- (13) Park, J.-S.; Jeong, J. K.; Mo, Y.-G.; Kim, H. D.; Kim, C. J. *Appl. Phys. Lett.* **2008**, *93*, 033513.
- (14) Barquinha, P.; Pimentel, A.; Marques, A.; Pereira, L.; Martins, R.; Fortunato, E. *J. Non-Cryst. Solids* **2006**, *352*, 1749–1752.
- (15) Lee, S. Y.; Kim, D. H.; Chong, E. Y.; Jeon, W.; Kim, D. H. *Appl. Phys. Lett.* **2011**, *98*, 122105.
- (16) Kang, D.; Lim, H.; Kim, C.; Song, I.; Park, J.; Chung, J.; Park, Y. *Appl. Phys. Lett.* **2007**, *90*, 192101.
- (17) Wang, Y.; Sun, X. W.; Goh, G. K. L.; Demir, H. V.; Yu, H. Y. *IEEE Trans. Electron Devices* **2011**, *58*, 480–485.
- (18) Jeong, J. K.; Yang, H. W.; Jeong, J. H.; Mo, Y.-G.; Kim, H. D. *Appl. Phys. Lett.* **2008**, *93*, 123508.
- (19) Park, J.-S.; Jeong, J. K.; Chung, H.-J.; Mo, Y.-G.; Kim, H. D. *Appl. Phys. Lett.* **2008**, *92*, 072104.
- (20) Oh, H.; Ko Park, S.-H.; Hwang, C.-S.; Yang, S. H.; Ryu, M. K. *Appl. Phys. Lett.* **2011**, *99*, 022105.
- (21) Jeong, J. H.; Yang, H. W.; Park, J.-S.; Jeong, J. K.; Mo, Y.-G.; Kim, H. D.; Song, J.; Hwang, C. S. *J. Electrochem. Soc.* **2008**, *11*, H157–H159.
- (22) Kwon, D. W.; Kim, J. H.; Chang, J. S.; Kim, S. W.; Kim, W. D.; Park, J. C.; Song, I. H.; Kim, C. J.; Jung, U. I.; Park, B. G. *Appl. Phys. Lett.* **2011**, *98*, 063502.
- (23) Ahn, B. D.; Shin, H. S.; Kim, H. J.; Park, J.-S.; Jeong, J. K. *Appl. Phys. Lett.* **2008**, *93*, 203506.